Enhancing fluorescent response of immunosensing by a dielectrophoresis chip with transparent electrodes and microcavities array

Cheng-Hsin Chuang, Jing-Wei Ju, Yao-Wei Huang

Department of Mechanical Engineering, Southern Taiwan University of Science and Technology, Tainan, Taiwan
E-mail: chchuang@mail.stust.edu.tw

Published in Micro & Nano Letters; Received on 18th July 2013; Accepted on 26th July 2013

Microelectrodes used in dielectrophoresis (DEP) chips are mostly made of metal materials; however, the metal electrodes can induce extra background noise as observed in a fluorescence microscope. Currently, the fluorescent response still dominates the indicators of immunoassays; therefore it is important to eliminate the extra background noise of the fluorescence response generated by metal electrodes for an immunosensor. In this reported study, a transparent conductive material, indium tin oxide (ITO), was employed in the fabrication of DEP electrodes, and the fluorescent responses of a DEP chip with transparent electrodes were compared with an identical DEP chip with conventional Au electrodes during an immunoassay. According to the experimental results, the enhancement of the fluorescent response of the DEP chip with ITO electrodes was greater than the values of the DEP chip with Au electrodes; about 1.57 times and 1.44 times for the immunosensing of 10 and 1 nm bovine serum albumin (BSA), respectively. In addition, by applying the DEP force during the immunosensing, the fluorescent response was also enhanced because of the condensation ability to BSA by the DEP force. Consequently, a DEP chip with transparent ITO electrodes and a microcavities array has been demonstrated, and the background noise of the fluorescence response can be eliminated to enhance the sensitivity of immunosensing.

1. Introduction: Immunoassays are biochemical tests used to detect blood or body fluid using an immunological reaction. Immunoassays are highly sensitive and specific because of the use of antibodies and purified antigens as reagents. A fluorescent label is usually utilised as an indicator to measure the formation of antibody–antigen complexes in an immunoassay. Recently, many researchers have tried to employ microfluidic techniques for developing the immunosensors, such as an immunosensor with a microchannel and microelectrodes for enzyme immunosensing based on electrochemical detection [1], an impedance sensor for bacteria detection based on biofunctional magnetic beads conjugated with antibodies [2], a surface modified gold-coated immunosensor for bacterium detection [3] and the employment of surface modified gold nanoparticles (NPs) for cancer biomarkers [4–6]. Although NPs have been utilised as the probes for immunosensing because of such advantages as their high surface-to-volume ratio, adequate size for most molecules, size-dependent properties and possible suspension, determining how to manipulate NPs to a predetermined position and in an array manner is still a task for integration with microfluidic devices.

Magnetic force is a common driving force for the rapid collection of magnetic NPs. Biofunctional magnetic beads could be captured in the target area by an externally positioned magnet [7–9], but the chip requires a magnet outside the device, which is difficult to integrate with the MEMS process and to achieve a microarray. Recently, the feasibility of NP manipulations by the dielectrophoresis (DEP) method has been demonstrated for different kinds of sensor fabrication, such as thermal sensors [10], humidity sensors [11] and immunosensors [12, 13]. According to these papers, the pattern of electrodes and the applied AC signals resulted in various NP assemblies. However, in these DEP chips, the electrode is always made of an opaque metal such as Au, Pt, Cu etc. In our prior work [14], we observed that the Au electrodes in the DEP chip could induce background noise in the fluorescence response, which reduced the sensitivity of immunosensing. Recently, Yasukawa and co-workers [15] employed a transparent conductive layer, indium tin oxide (ITO), as the top DEP electrode and modified the ITO surface for the fluorescent observation of immunoassay. In this reported study, ITO glass was patterned for fabricating the DEP electrodes. Also, bio-modified NPs were introduced to the DEP chip and immobilised on a dot electrode array by DEP force, for immunosensing based on fluorescent responses. By controlling the identical sensing conditions and DEP chips, we could compare the fluorescent response of an ITO-electrode chip and a Au-electrode chip experimentally. This study may provide a new DEP chip fabrication method, and dot-pattern fluorescence results of immunosensing.

2. Simulation of a non-uniform electric field: The time-averaged dielectrophoretic force acts on a spherical particle, immersed in a medium and exposed to a spatially non-uniform electric field. The dipole component of the DEP force is

$$\boldsymbol{F}_{\mathrm{DEP}} = 2\pi\varepsilon_{\mathrm{m}}R_{\mathrm{p}}^{3}\mathrm{Re}[K(\omega)]\nabla E_{\mathrm{rms}}^{2} \tag{1}$$

where ε_{m} is the electrical permittivity of the surrounding medium, R_{p} is the radius of the particle and ω is the angular frequency

$$\left|\nabla E_{\mathrm{rms}}^{2}\right| = \sqrt{\nabla E_{x}^{2} + \nabla E_{y}^{2} + \nabla E_{z}^{2}}$$

is the gradient of the square of the applied electric field magnitude, and $K(\omega)$ is the frequency-dependent Claussius-Mosotti (CM) factor for a dielectric uniform sphere, such as a bead. In a non-uniform electric field, the nature of the DEP force whether positive or negative is dependent on the CM factor; the magnitude of the DEP force is determined by the imposed electrical field at the particle position, as well as by the size of the particle itself. In our previous work, we demonstrated that the bio-modified NPs with an average diameter of 30 nm could be trapped and immobilised onto the dot electrodes by positive DEP force [13]. This Letter further employed a thick photoresist layer (SU-8) to form the microcavities array on the DEP electrode and cover the wiring, consequently a dot-electrode array can be achieved and the fluorescence response can be quantified based on the same area of the dot electrode.

A three-dimensional (3D) model of the present DEP chip with microcavities was simulated by the COMSOL Multiphysics (COMSOL, Sweden), and the parameters for the medium and SU-8 are listed in Table 1. The structure of the DEP chip consisted of an ITO top electrode, a flow chamber 50 µm in height, SU-8 microcavities with 20 µm diameter and 10 µm thickness on the bottom electrodes' surface and the bottom electrodes made of Au/ITO, as shown in Fig. 1*a*. For the electrical boundary condition, the top electrode and bottom electrode were set to grounded and 10 V at 10 kHz, respectively. The total number of mesh elements in the simulation model was about 272 211, as determined by the convergence test.

The purpose of the bottom electrodes was to trap the nanoprobes into the microcavities by positive DEP force. As is known, the DEP force is valid for a non-uniform electric field, E, and proportional to the gradient of the square of the electric field, ∇E^2. Hence, E and ∇E^2 were calculated by the simulation tool, as shown in Figs. 1*b* and *c*, respectively. According to the simulation results, the highest electric field occurred near the edge of the bottom electrode surface; conversely, the lowest electric field existed in the flow chamber. Therefore these nanoprobes can be attracted to the electrode by positive DEP. Furthermore, the highest values of the electric field and the gradient of the square of the electric field were 9.38×10^6 V/m and 8.45×10^{19} V^2/m^3 which are both greater than the values ($E = 6.63 \times 10^5$ V/m and $\nabla E^2 = 3.65 \times 10^{17}$ V^2/m^3) indicated in our previous work [13]. Consequently, a DEP chip consisting of a SU-8 microcavity could enhance the DEP force and provide rapid trapping of nanoprobes into the microcavity.

Table 1 Material properties for simulation

Properties/materials	Medium	SU-8
density ρ, kg/m^3	1000	1194
conductivity σ, S/m	2×10^{-4}	1×10^{-14}
relative permittivity, ε	80	4

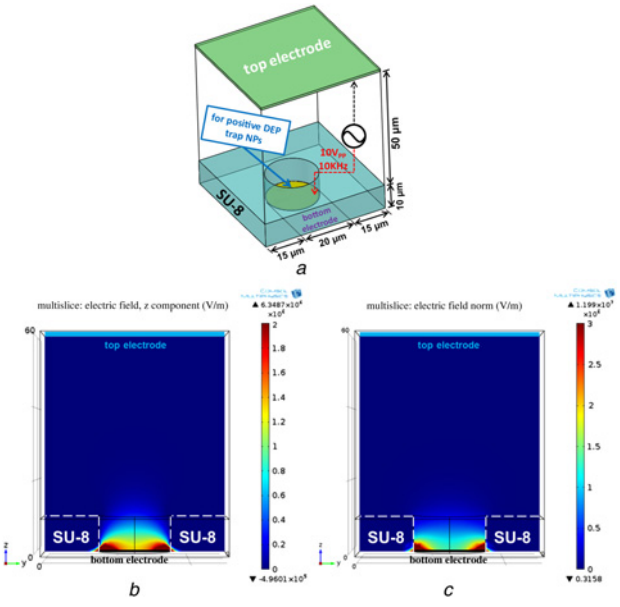

Figure 1 *3D model of DEP chip with top and bottom electrodes and SU-8 microcavity; contour of electric field; contour of* ∇E^2
a 3D model of DEP chip
b Contour of electric field
c Contour of ∇E^2

3. Materials

3.1. Preparation of nanoprobes: In this work, we used low-cost commercial aluminium oxide NPs (Al_2O_3-NPs) from Evonik Degussa Taiwan Ltd (AEROXIDE® Alu C, Evonik Degussa). The Al_2O_3-NPs had an average diameter of 20 nm. To modify the surfaces of Al_2O_3-NPs with the amino groups (–NH_2), a conventional modification scheme was utilised by using the silane solution (3-aminopropyltrimethoxysilane, MERCK) and the following steps. First, 3 g of ethanol with 95% concentration, 1.5 g deionised (DI) water (Millipore Direct-Q® 3 system) and 1.25 g of silane solution were mixed and stirred at room temperature for 3 h. Secondly, the 2.7 g Al_2O_3-NPs and 100 g 95% ethanol were mixed by a Homo Mixer (HM-302, HSIANGTAI) for 10 min. Then, these two solutions were mixed and stirred at double-boiling at 70°C for 3 h. Next, the suspended NPs were precipitated after three times centrifuging (CN-2200, HSIANGTAI) at 4000 rpm for 10 min. The sedimentary NPs were pipetted out and baked at 60°C for 12 h. Afterwards, the solid nanopowders modified with silane on the surfaces could be obtained for the preparation of two weight percentages of NP suspensions in 10 cc of DI water. To bind the antibody on silane-modified NPs, 0.5 cc of glutardialdehyde (glutaraldehyde 25% aqueous solution, MERCK) and 1 cc of bovine serum albumin (BSA)-antibody (GTX29092, GeneTex®, Inc.) were sequentially added into the 10 cc of silane-modified NP suspension and stirred for 30 min each. Finally, the antibody-Al_2O_3-NPs were prepared and utilised as the nanoprobes in the immunosensing.

3.2. Fabrication of the DEP chip: In our experiments, two DEP chips with different bottom electrode layers, a Au layer and an ITO layer, were fabricated by the same photomasks and processes. The fabrication processes consisted of three parts, as shown in Fig. 2. First, five bottom line electrodes for trapping nanoprobes were patterned by standard photolithography and wet etching on a 25×70 mm^2 ITO glass, as shown in Fig. 2*a*; the line width of the bottom electrode was 40 µm and the layout of five bottom electrodes are shown in Fig. 3. Secondly, a SU-8 microcavities array was patterned with a dot-array photomask, as shown in Fig. 2*b*. The diameter, spacing and depth of the microcavity array were designed as 20, 100 and 10 µm, respectively. A total of 5 by 5 microcavities were fabricated on the five bottom line electrodes. The last part was a rectangular flow chamber, with the dimensions of $W \times L \times H = 4$ mm $\times$ 30 mm $\times$ 50 µm, formed by twin adhesive taped to ITO glass, as shown in Fig. 2*c*. The finished DEP chip is shown in Fig. 2*d*.

4. Experimental methods

4.1. Experimental setup: The experimental setup is shown in Fig. 3. A syringe pump (KDS-100, KD Scientific) was utilised to control

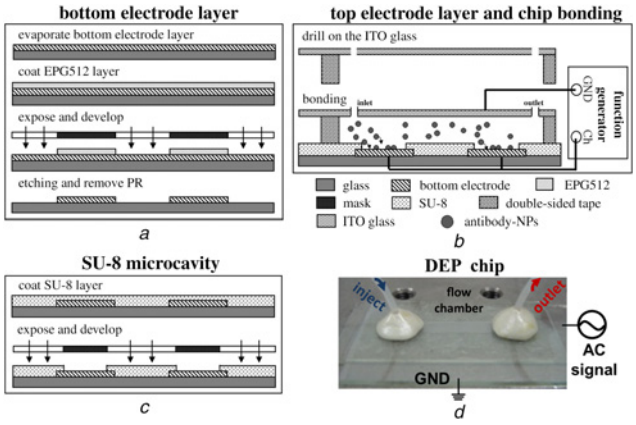

Figure 2 *Fabrication process of DEP chip for trapping and immunoassay*

doi: 10.1049/mnl.2013.0439

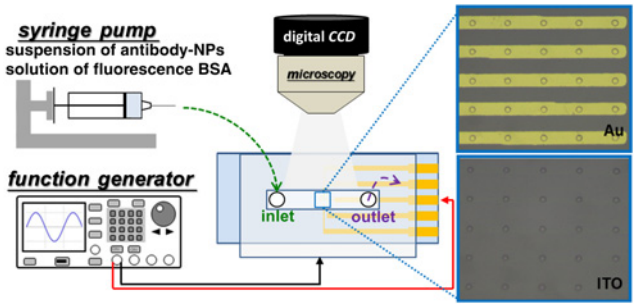

Figure 3 *Experimental setup for DEP manipulation of antibody-Al_2O_3-NPs*

the flow rate of suspension, and the AC signal was generated by a function generator (AFG3022, Tektronix) for DEP trapping of antibody-Al_2O_3-NPs. A digital CCD (XC10, Olympus) camera was mounted on a biological microscope (BX51, Olympus) for monitoring the DEP force acting on the nanoprobes, and was utilised to capture the fluorescent images of the immunosensing results. In the experiments, two kinds of DEP chip with Au and ITO bottom electrodes were employed for the comparison of fluorescence response, as shown in the optical images in Fig. 3. To obtain consistent DEP results, the conductivity and pH value of the nanoprobes suspension were controlled in a proper range of 160–180 µs/cm and 6.6 by a conductivity meter (SC-170, Suntex) and a pH meter (TS-100, Suntex), respectively. In addition, each fluorescence image was exposed for 2000 ms and further analysed using fluorescent analysis software (Quantity One, BIO-RAD, USA) based on the same marked area. Consequently, we could evaluate the fluorescence response of immunosensing on the DEP chips with opaque and transparent bottom electrodes individually.

4.2. Experimental procedure: The experimental procedure involved three steps. First, the nanoprobes suspension was pumped into the flow chamber by a syringe pump at 10 ml/h flow rate for about 1 min to fill the flow chamber. Then, a continuous slow flow rate at 0.1 ml/h was pumped into the flow chamber for the trapping of nanoprobes. After the flow stabilised, the nanoprobes were trapped into the microcavities array by positive DEP force as an applied AC signal with 10 V_{PP} at 10 kHz to the bottom electrodes for 15 min, as indicated in Fig. 4*a*. After the trapping process, the AC signal was stopped, and a continuous flush at 10 ml/h applied to the flow chamber for 5 min so that the non-immobilised nanoprobes could be purged to the waste reservoir, as indicated in Fig. 4*b*. In the final step, a fluorescent labelled BSA suspension was subsequently introduced to the DEP chip for immunosensing, when the BSA suspension is full we stopped the flow and began immunosensing, as indicated in Fig. 4*c*. Meanwhile, a digital CCD mounted on a biological microscope captured fluorescence images every 10 min within 1 h. Then, the fluorescent intensity of each image with a specific marked area was calculated by image processing software. To eliminate the factor of the amount of NPs trapped on electrodes, we normalised the variation of fluorescent intensity between 0 and 60 min by the intensity at 0 min, that is, $\Delta I/I_0$, where $\Delta I = I_{60} - I_0$, and called $\Delta I/I_0$ as the enhancement ratio of fluorescent intensity. Thus, the enhancement ratios for different kinds of DEP chip and with/without DEP force as immunosensing can be evaluated by averaging the values from ten dot electrodes.

5. Experimental results and discussion: Prior to obtaining the immunosensing results, the nanoprobes were trapped in the microcavities array by Au bottom electrodes and ITO electrodes. In the DEP trapping procedure, the AC signal was applied to nos

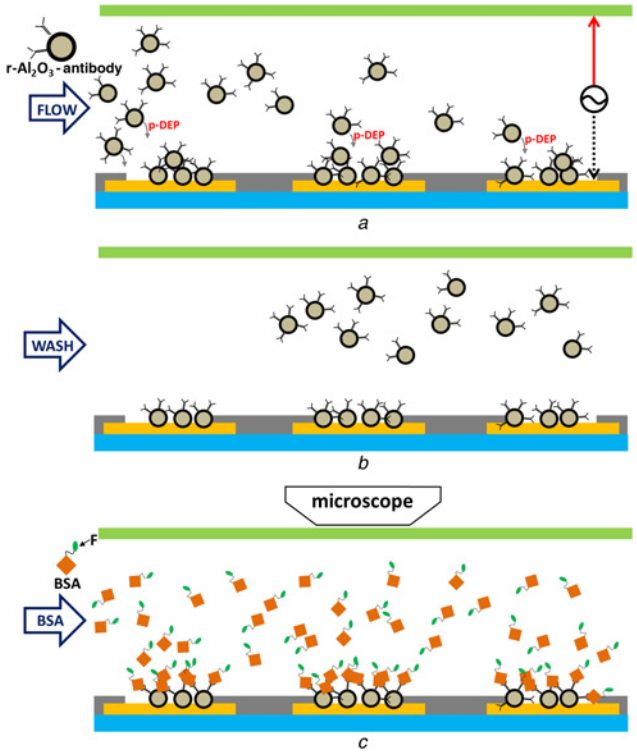

Figure 4 *Schematic diagram of experimental steps*
a Trapping and immobilising antibody-Al_2O_3-NPs into microcavities array
b Flushing DI water into chamber
c Injecting fluorescent-label BSA for immunosensing

1, 2, 4 and 5 bottom electrodes for 15 min; only no. 3 bottom electrode did not apply the AC single as a reference electrode on the DEP chip, as shown the fluorescent images (filter 468 nm) in Figs. 5*a* and *d*. There were low fluorescent responses in the nos 1, 2, 4 and 5 electrodes except no. 3 electrode, which means these nanoprobes indeed immobilised in the microcavities by DEP force. Note that the low-level fluorescence resulted from the binder material of the nanoprobes, glutardialdehyde, which can be excited by a mercury lamp using fluorescent microscopy. In addition, the Au electrodes were still observed in the fluorescent images, as shown in Fig. 5*d*; therefore the Au electrode could induce the background value of fluorescence intensity as immunosensing. Conversely, the transparent electrode would not induce the background value of fluorescence intensity.

As the nanoprobes were immobilised in the microcavities, the DEP chip was ready for measuring the immunoreaction with fluorescent protein. In this study, fluorescent protein AF488-BSA from Molecular-Probes® (Bovine Serum Albumin AF488-conjugated) was conjugated with antibodies to demonstrate immunosensing based on fluorescent intensity. The immunofluorescence images for the DEP chip with ITO bottom electrodes as 10 nm protein suspension were syringed into the flow chamber ($t = 0$) and incubated for 1 h, are illustrated in Figs. 5*b* and *c*, respectively; the results of the DEP chip with Au bottom electrodes are described as Figs. 5*e* and *f*. Note that these four images were adjusted by black balance for the contrast enhancement. The black balance is used to select a black or dark area in the image for black balance reference. In our cases, we selected an area in the no. 3 bottom electrode as the black balance reference where no nanoprobes were immobilised on the electrode.

Generally, the fluorescent intensities of both the ITO-electrode chip and the Au-electrode chip were enhanced after 60 min sensing time in the immunoassay. In addition, the fluorescence intensities of nos 1 and 2 line electrodes were displayed relatively

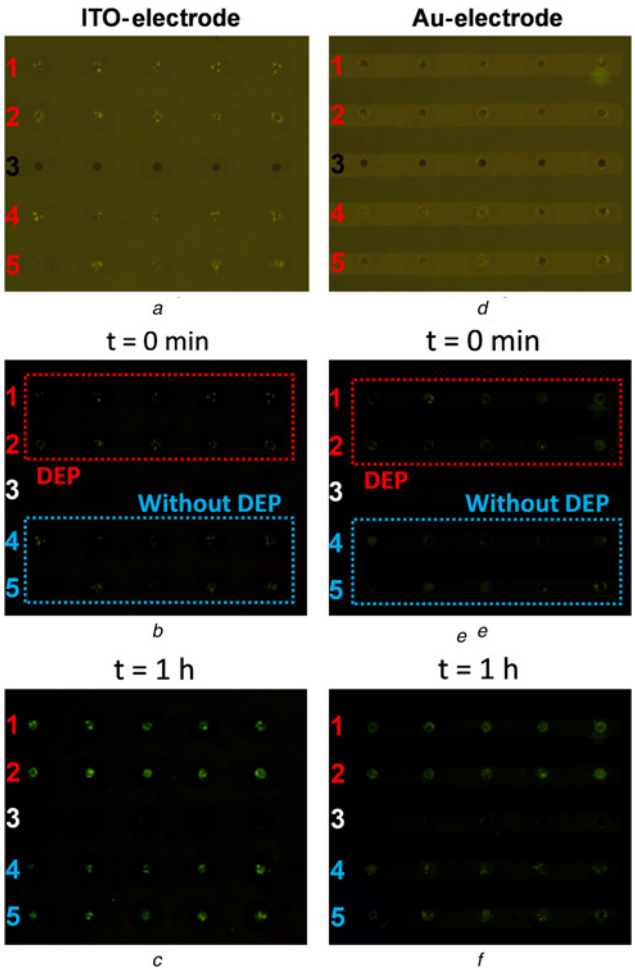

Figure 5 *Comparison between transparent (ITO) electrodes and opaque (Au) electrodes as immunosensing at 0 min and after 1 h*
a–c Fluorescent images of ITO electrodes
d–f Fluorescent images of Au electrodes

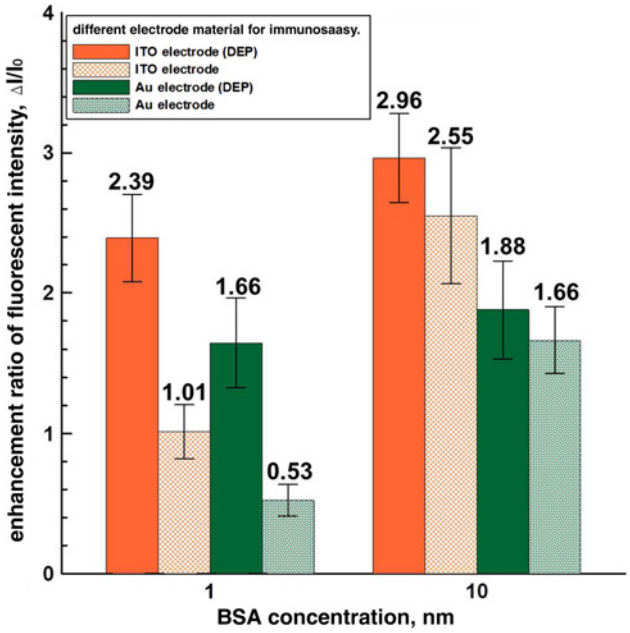

Figure 6 *Enhancement ratio of fluorescence intensity for 10 nm and 1 nm BSA concentration after 1 h immunosensing with/without applying DEP force*

greater than the cases of the nos 4 and 5 line electrodes for the DEP chip with ITO and Au electrodes, as shown in Figs. 5*c* and *f*, respectively. This phenomenon can be attributed to DEP effects as immunosensing because we applied the DEP force only on nos 1 and 2 line electrodes with 10 V_{PP} at 10 kHz for 1 h sensing time. Consequently, we could evaluate the DEP effect on immunosensing by comparing different electrodes in the single chip. As for the results indicated in Fig. 6, the enhancement ratio of fluorescence intensity for immunosensing of 10 nm BSA is on average greater than 1 nm BSA because of the concentration of fluorescent protein being higher. Furthermore, the enhancement ratio of fluorescence intensity for the DEP chip with ITO electrodes is generally greater than the value for the DEP chip with Au electrodes under the same protein concentration. For example, the enhancement ratio of the ITO-electrode chip for immunosensing of 10 nm BSA under applying DEP force is 2.96, which is 1.57 times greater than the value of the Au-electrode chip (1.88). For the cases of 1 nm BSA, the difference of the enhancement ratio between the ITO-electrode chip and the Au-electrode chip is about 1.44 times. Consequently, a DEP chip employing transparent electrodes could really enhance the fluorescent response of immunosensing.

For the DEP effect on immunosensing, the enhancement ratios of cases with DEP force are higher in total than the cases without DEP force. In addition, the increment of the enhancement ratio between with and without DEP for 1 nm BSA immunosensing is higher than 10 nm BSA immunosensing. For example, if we divide the enhancement ratio of an ITO-electrode chip with DEP, by the value without DEP for 1 nm and 10 nm BSA individually, the increment of 1 nm is 2.37 times, which is higher than 1.16 for the 10 nm case. Therefore applying DEP force as immunosensing can condense the protein to the microcavity by positive DEP force, and increase the binding ratio of antibody–protein interaction. Also, the influence of the DEP force is more significant for a lower concentration of protein suspension.

6. Conclusions: In the work reported in this Letter, we have developed an immunosensor for the immobilisation of antibody-NPs in a SU-8 microcavities array and evaluated the enhancement of fluorescence intensity for the immunosensing using transparent electrodes and DEP force. According to the experimental results, the fluorescence response of an ITO-electrode chip is about 1.5 times greater than that of a Au-electrode chip, and the influence of DEP force as immunosensing is more significant in low-concentration protein suspension. In general, transparent electrodes are not only suitable for DEP manipulation of NPs, but also enhance the contrast of fluorescent response for immunosensing. Consequently, a DEP chip with transparent electrodes and a microcavities array could provide higher sensitivity of immunoassay and more quantifiable evaluation of fluorescent response. We will employ this platform technique to fabricate a multi-antibody array in a single chip in the near future.

7. Acknowledgments: This study was financially supported by the National Science Council Taiwan (Project No. NSC 101-2221-E-218 -020 and NSC 101-2218-E-218 -004). The authors thank the Optoelectronics, Nanotechnology Research Center and Conducting Polymer Laboratory in Southern Taiwan University for the use of the MEMS and material process facilities.

8 References

[1] Raba J., Messina G.A., Panini N.V., Martinez N.A.: 'Microfluidic immunosensor design for the quantification of interleukin-6 in human serum samples', *Anal. Biochem.*, 2008, **380**, pp. 262–267
[2] Chan K.Y., Ye W.W., Zhang Y., *ET AL.*: 'Ultrasensitive detection of E. coli O157:H7 with biofunctional magnetic bead concentration

doi: 10.1049/mnl.2013.0439

via nanoporous membrane based electrochemical immunosensor', *Biosens. Bioelectron.*, 2013, **41**, pp. 532–537
[3] Park M.K., Park J.W., Oh J.H.: 'Optimization and application of a dithiobis-succinimidyl propionate-modified immunosensor platform to detect *Listeria monocytogenes* in chicken skin', *Sens. Actuator B, Chem.*, 2012, **171–172**, pp. 323–331
[4] Zhang H., Liu L., Fu X., Zhu Z.: 'Microfluidic beads-based immunosensor for sensitive detection of cancer biomarker proteins using multienzyme-nanoparticle amplification and quantum dots labels', *Biosens. Bioelectron.*, 2013, **42**, pp. 23–30
[5] Hsu W.T., Hsieh W.H., Cheng S.F., *ET AL.*: 'Integration of fiber optic-particle plasmon resonance biosensor with microfluidic chip', *Anal. Chim. Acta*, 2011, **697**, pp. 75–82
[6] Lee S.H.S., Hatton T.A., Khan S.A.: 'Automated microfluidic processing platform for multiplexed magnetic bead immunoassays', *Microfluid. Nanofluid.*, 2011, **11**, pp. 429–438
[7] Sasso L.A., Johnston I.H., Zheng M., Gupte R.K., Ündar A., Zahn J.D.: 'Automated microfluidic processing platform for multiplexed magnetic bead immunoassays', *Microfluid. Nanofluid.*, 2012, **13**, pp. 603–612
[8] Wang J.H., Cheng L., Wang C.H., Ling W.S., Wang S.W., Lee G.B.: 'An integrated chip capable of performing sample pretreatment and nucleic acid amplification for HIV-1 detection', *Biosens. Bioelectron.*, 2013, **41**, pp. 484–491
[9] Leung S.L., Li M., Li W.J., Mai J.D.: 'Gold nano-particle-based thermal sensors fabricated using microspotting and DEP techniques', *Sens. Actuator A, Phys.*, 2012, **178**, pp. 32–39
[10] Chen L., Zhang J.: 'Capacitive humidity sensors based on the dielectrophoretically manipulated ZnO nanorods', *Sens. Actuator A, Phys.*, 2012, **178**, pp. 88–93
[11] Shew B.Y., Chu H.C., Chen C.K., *ET AL.*: 'Enhancement of specific cell-capture efficiency using a reversible dielectrophoresis field', *Sens. Actuator A, Phys.*, 2010, **163**, pp. 128–137
[12] He X., Hu C., Guo Q., Wang K., Li Y., Shangguan J.: 'Rapid and ultrasensitive Salmonella Typhimurium quantification using positive dielectrophoresis driven on-line enrichment and fluorescent nanoparticles label', *Biosens. Bioelectron.*, 2013, **42**, pp. 460–466
[13] Tokonami S., Iwamoto M., Hashiba K., Shiigi H., Nagaoka T.: 'Fabrication of a highly sensitive sensor electrode using a nano-gapped gold particle film', *Solid State Ion.*, 2006, **177**, pp. 2317–2320
[14] Chuang C.H., Huang Y.W.: 'Condensation of fluorescent nanoparticles using a DEP chip with a dot-electrode array', *Microelectron. Eng.*, 2012, **97**, pp. 317–323
[15] Ramón-Azcón J., Yasukawa T., Lee H.J., *ET AL.*: 'Competitive multi-immunosensing of pesticides based on the particle manipulation with negative dielectrophoresis', *Biosens. Bioelectron.*, 2010, **25**, pp. 1928–1933